XIX IMEKO World Congress
Fundamental and Applied Metrology
September 6−11, 2009, Lisbon, Portugal

EVALUATION OF AN ASYNCHRONOUS SAMPLING CORRECTION TECHNIQUE SUITABLE FOR POWER QUALITY MEASUREMENTS

Paul Clarkson [1], *Paul Wright*[1]

[1] National Physical Laboratory, Teddington, UK, paul.clarkson@npl.co.uk

Abstract − The accurate measurement of many power quality parameters using digital sampling techniques relies on synchronisation between the sampling system and the signal under analysis. If synchronisation is not available measurement errors result due to the difference in frequency of the digitised signal and that expected and based on the sampling clock of the measurement system.

A method is presented of correcting for this lack of synchronisation. This method relies on a time domain interpolation technique to modify the sampling rate of the captured signal in software. In order to find the correct sampling rate a scanning technique is used which requires some method of assessing the lack of synchronisation and associated error in the analysis of the signal. A number of methods of achieving this are presented and compared. The suitability of the algorithm for power quality measurements under noisy conditions is assessed.

Keywords: asynchronous sampling, power quality, spline interpolation.

1. INTRODUCTION

In the laboratory, measurements of power quality parameters described in IEC 61000-4-30 [1] are relatively straightforward. Digital sampling techniques can be used and the sampling clock can usually be synchronised to the signal under analysis. Power quality measurements on the electricity supply network are considerably more difficult. There is often no means of synchronising the measurement system with the signals to be analysed, which leads to errors in the measurements of parameters that rely on an assumed frequency, e.g. harmonics obtained from the DFT and flicker, which relies on filters which are designed based on a given sampling rate and frequency. Further, measurements conducted in the field, outside of the laboratory are corrupted by noise, making analysis more difficult.

The digital measurement and analysis of many power quality measurements relies on an assumed periodicity in the sampled waveform. For example, in the case of harmonics measurements, if the period of the waveform is a non-integer number of samples the energy contained in the harmonic bins leaks across the spectrum. This leakage is due to a difference in the sampling rate from that of the ideal rate, which would result in an integer number of samples, i.e.

$$f_s \neq f \cdot T \tag{1}$$

where f_s is the sampling rate in Hz, f is the signal frequency and T is the period of the signal in samples. The error in sampling rate, Δ, is given by equation (2), as follows

$$\Delta = f_s - f \cdot T \tag{2}$$

A number of techniques of correcting for the error have been proposed. The majority of these focus on frequency domain interpolation and windowing techniques [2], [3] to correct for the leakage in harmonic measurement. Others propose methods of correcting for the error e.g. [4], but some of these assume that the error Δ, is known and do not provide a method of finding the error. Time domain interpolation techniques have also been used but do not necessarily provide a definitive method of determining the corrected signal, e.g. [5]. Other techniques rely on synchronisation hardware or a modification of the sampling rate and re-sampling at the new rate [6].

Another promising technique is based on a modified version of the sine fitting procedure described in [7] and [8]. This method, which has yet to be published, was developed at the Metrology Institute of the Republic of Slovenia (MIRS) and the Slovenian Institute of Quality and Metrology (SIQ). Comparisons between the method in this paper and that developed at MIRS/SIQ have been carried out with colleagues at MIRS/SIQ and it is hoped that these comparisons will be published at a later date.

The technique described in the next section of this paper is intended to be suitable for a wide variety of power quality measurements, and to be applied entirely in software requiring no hardware modifications such that any sampled dataset can be analysed. It relies on a cubic spline interpolation of the signal in a similar manner to [5], which is used to modify the sampling rate in software. The interpolation is shown to be sufficiently accurate for the reproduction and correction of the signal. A scanning technique is then used where the sampling rate is swept across a range of frequencies and an assessment is made of the correctness of the modified sampling rate using a cost function, which is minimised. The choice of cost function is dependent on the expected characteristics of the signal to be analysed and on the power quality parameter to be measured. Several cost functions are described in Section 3, which are intended to be suitable for the measurement of harmonics for periodic, stationary waveforms. The results of

ISBN 978-963-88410-0-1

comparisons with these cost functions are presented in Section 4.

Further work is required to improve the performance of the algorithm under noisy conditions and to expand on the method for the measurement of other power quality parameters and waveform types (e.g. waveforms modulated in amplitude and frequency). This work is focussed mainly on the improvement of the cost functions.

2. INTERPOLATION AND SCANNING METHOD

2.1. Description of the algorithm

The method can be broken down into a number of steps:

1. An initial range of estimated frequencies (e.g. a range of 2 Hz), f_R, is selected for the frequency scan. This is centred around the ideal frequency (e.g. 50 Hz), f_s/T, where f_s is the sampling rate used and T is the expected period of the signal in samples. The initial estimate of frequency, f_e, is set to (f_s/T)-$(f_R/2)$. The correction factor, C, for the sampling rate is computed using the following equation.

$$C = \frac{f_s}{T \cdot f_e} - 1 \qquad (3)$$

   The initial step size in frequency and a threshold for the minimum desired frequency resolution, λ, are selected.
2. The splines of the waveform are computed. The algorithm used to compute the splines and interpolate the sampled signal is taken from [9].
3. Each of the N sampled data points, S(i), is interpolated between adjacent samples S(i) and S(i+1) or S(i-1), hence effectively changing the sampling rate, to obtain an estimate of the signal at a new sampling rate, modified by the correction factor, C, such that S(i) is replaced with s′(i·(1+C)), which is obtained by interpolation.
4. An estimate of the error in the signal is obtained using one of the cost functions described in Section 3 below.
5. The estimate of the frequency is increased by a chosen amount, Δf (say 0.1 Hz), the correction factor C is computed from the new frequency estimate and steps 2 and 3 are repeated. This step is repeated until a minimum is reached for the cost estimate obtained in step 3.
6. Once a first estimate for the frequency has been obtained a finer scan can be used either side of this estimated value. So, say 50.2 Hz was found as the estimated rate from the first scan. A new scan can then be performed starting at 50.15 Hz, increasing in steps of 0.01 Hz, until a minimum is again found for the cost function. Finer and finer scans can be used to obtain more and more accurate estimates, until the desired frequency resolution, λ, is obtained.

The algorithm is summarised in the flowchart in Figure 1 below.

The success of the algorithm is limited by the quality of the interpolation and of the suitability of the chosen cost function used to estimate the error in the signal due to asynchronous sampling. The next subsection addresses the former of these criteria and Section 4 assesses the latter by comparing various cost functions. The cost functions can be assessed without using interpolation by simulating signals sampled at the modified sampling rates used during the scanning procedure. This is explained further in Section 4.

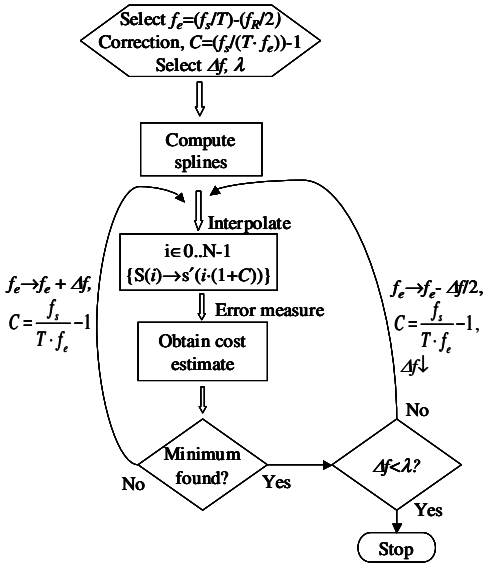

Fig. 1. Algorithm flowchart.

2.3. Assessment of the quality of the interpolation

It is very important that the interpolation provides an accurate representation of the sampled signal. The assessment of the accuracy of the interpolated signal can be achieved in simulation by comparing the interpolated signal, corrected for a known error in the signal frequency, with that of a simulated signal of the ideal frequency (i.e. the frequency which results in an integer number of samples per period).

It can be shown that the accuracy of the interpolation is sufficient to within 150 ppm of RMS component amplitude for signal components having frequencies of less than around f_s/12.5, improving to within 0.1 ppm for components having frequencies of less than f_s/100. As such all harmonics of a 50 Hz sinusoidal waveform composed of harmonics up to the 40th (important for power quality work) can be recovered accurately to within 150 ppm for the higher order harmonics and within 0.1 ppm for the lower order harmonics for a sampling rate of 25 kHz. Further, the RMS difference between samples for the corrected interpolated waveform and that sampled at the ideal rate is less than 5 ppm of RMS signal amplitude for a waveform composed of harmonics up to f_s/12.5 and less than 0.5 ppm for a waveform composed of harmonics up to f_s/25.

Performance under noise is more difficult to assess, but it can be shown in simulation that any deviations in the corrected signal from that of the ideal signal are within the

added noise, apart from the residual errors described in the previous paragraph. The results presented in Section 4 show that there is some deviation in the recovered frequency at higher noise levels when using interpolation compared to that when re-sampling simulated waveforms at different sampling rates, but provided an appropriate cost function is chosen, the resulting errors in the harmonic amplitudes are acceptable for the level of added noise.

3. METHODS OF ERROR ASSESSMENT

As explained earlier, in order to find the ideal sampling rate for a given signal an appropriate cost function must be used to determine the error in the analysis of the signal caused by asynchronous sampling. Five cost functions are suggested here, all of which should give a minimum when the ideal sampling rate is found.

The following measures are subjective and rely on a certain amount of prior knowledge about the signal to be analysed. They are specifically selected for harmonic analysis of stationary waveforms. For other types of waveform or power quality measurement parameters different cost functions would be required. Modifications are also required to improve the performance under noisy conditions. These modifications are currently under development.

The performance of the algorithm with each of the cost functions under various conditions is assessed in Section 4.

3.1. Interharmonics and high harmonics sum

Asynchronous sampling results in spectral leakage, therefore a measure of the amount of leakage can provide an assessment of the deviation in sampling rate from ideal. An estimate must first be made of the expected spectral characteristics of the signal under analysis. A Discrete Fourier Transform (DFT) of the signal is performed and the sum of the harmonics and interharmonics that are not expected to occur is calculated. This sum is then divided by the fundamental amplitude to obtain the error metric.

The number of cycles to use for the DFT and the number of harmonics to use in the cost function depend on the expected characteristics of the signal under analysis and are the subject of further investigation. For the example given in Section 4 only interharmonics up to the 40th harmonic are minimised and not harmonics.

3.2. Phase drift

If a signal is sampled asynchronously then the difference in frequency of the signal from the assumed frequency will result in a phase drift with time on a cycle-by-cycle basis.

The phase of the fundamental is computed using Fourier analysis for two subsets of the sampled signal, spaced an integer number of estimated signal periods apart. The difference in phase of the two subsets is used as the cost measure.

The chosen length and separation of the two subsets depends on the characteristics of the signal under analysis. In an ideal case where the phase of the underlying signal is constant and any variation purely down to the error due to asynchronous sampling both should be maximised for best results, but the choice in a real situation would depend on how stable the underlying signal is assumed to be. Longer separations and subset lengths are more robust to noise, but more susceptible to errors due to frequency and phase variations in the signal.

A variation in phase with time is equivalent to a frequency offset. Therefore an estimate of the frequency error can be obtained by differentiating the measured phase with respect to time. The correction factor, C, defined above can then be calculated using the following equation.

$$C = \frac{f_s}{T \cdot f_e \cdot \left(1 + \frac{\Delta\phi \cdot T}{2\pi \cdot \Delta n}\right)} - 1 \qquad (4)$$

where $\Delta\phi$ is the phase difference between the two subsets and Δn is the time spacing in samples. f_e is set to f_s/T for the first iteration. Equation (4) is equivalent to the expression used in [6].

The spacing between the two subsets must obviously be kept below 2π radians, otherwise erroneous results would be obtained. Adjacent cycles can be used to estimate the initial frequency error and associated correction factor, followed by wider spacings for subsequent iterations.

This procedure leads to a much faster convergence of the algorithm than the scanning technique shown in Fig. 4. However, for the results in Section 4 the scanning technique is used in order to ensure consistency of approach for the comparison of cost functions.

3.3. Energy concentration

A function that is analogous to a simplified version of information entropy [10] can be applied to the Fourier series of the sampled signal to provide a measure of the concentration of the energy in the signal across the spectrum. A lower value should indicate that more energy is concentrated in fewer Fourier coefficients. The energy concentration can therefore provide an estimate of the amount of smearing or leakage across the spectrum.

The energy concentration measure, γ_e, is given by the following equation,

$$\gamma_e = \sum_{h=0}^{H-1} \frac{|X_h|}{\sum_{h=0}^{H-1} |X_h|^2} \qquad (5)$$

where X is the Fourier series of the sampled signal, h is the Fourier coefficient number and H is the number of Fourier coefficients.

3.4. Fundamental sidebands

This is a special case of the cost function in section 3.1, where only the amplitudes of the interharmonic sidebands near to the fundamental, divided by the fundamental amplitude, are used as the cost measure. The sidebands can also be used in conjunction with the phase drift method as described in [6].

3.5. Time series comparison

If the signal is assumed to be periodic then each cycle should be identical. The sampled signal is divided into two subsets of the same length having an integer number of cycles (based on the assumed frequency) and the difference between the subsets on a sample-by-sample basis is taken. The RSS sum of these differences is used as the cost measure. A similar argument applies to that used for the phase drift method described in Section 3.2 regarding the length and spacing of the subsets. The frequency resolution of the previous scan can be used to calculate the maximum allowable spacing.

4. RESULTS

Two signals were used to assess the performance of the algorithm. The first was a simple sine wave with no harmonics and the second a distorted waveform composed of harmonics up to the 40th with relative amplitudes and phases set to those in [11]. This waveform is based on the limits specified in IEC 61000-3-2 [12] for Class A equipment.

The waveforms were first simulated and analysed in software and the results of this analysis are shown in Section 4.1.

The undistorted sine wave and Class A waveform were then generated as real signals using two voltage sources and sampled using a 24-bit ADC. The undistorted sine wave was generated with a relatively high quality, calibrator grade voltage source and also using a 12-bit arbitrary waveform generator (ARB). The Class A waveform was generated using the ARB. A measurement of the generated signals was first made using synchronised sampling and the results were compared with those using asynchronous sampling with the correction technique. These results are shown in Section 4.2.

4.1 Results of simulations

For the simulations the frequency of the signal was set to 50.5685721561313 Hz. The signal was sampled at a rate of 25 kHz, such that the ideal period was 500 samples. The signal was 20 cycles long.

Five tests were performed on the Class A waveform using each of the cost functions defined in Section 3. The first test is on the simulated signal with no noise, this signal is unquantised apart from the 32-bit precision of the arithmetic. For the second the Class A waveform is quantised with 16-bit resolution. Pseudo random white noise of 0.1, 1 and 10 % of signal amplitude is then added for the other tests.

The modification to the sampling rate for the scanning procedure described in Section 2 above was carried out in two ways. The first was to interpolate between samples to achieve the modified sampling rate, as would be required for analysis with real waveforms. The second was to simulate the signal with the modified sampling rate.

The errors in estimated frequency recovered from the tests, obtained with each of the cost functions, are given in Table 1.

Comparisons of the errors in frequency estimate obtained when using interpolation to change the sampling rate and when using a re-sampled simulated signal, indicate that errors in recovered frequency are increased by the interpolation in noisy conditions. Much of the error is down to the cost function. Therefore the focus of future work will be on finding a cost function that is not so affected by noise and improving the interpolation method under noise.

Table 1. Frequency errors in ppm of nominal. Errors when re-sampling without using interpolation are shown in brackets.

Signal type \ Cost function	3.1	3.2	3.3	3.4	3.5
Unquantised	-6E-06 (-1E-07)	1E-04 (-1E-07)	-6E-06 (-1E-07)	-1E-07 (-1E-07)	-2E-05 (-1E-07)
Quantised	-3E-03 (1E-04)	-2E-02 (1E-04)	-3E-03 (1E-04)	-3E-03 (1E-04)	-6E-03 (1E-04)
0.1 % noise	0.09 (-0.01)	0.70 (0.78)	0.08 (-0.13)	1.00 (0.83)	0.01 (0.03)
1 % noise	0.9 (-0.1)	6.7 (7.4)	0.8 (-0.2)	9.6 (7.4)	0.1 (-0.1)
10 % noise	9.0 (-0.3)	67.3 (73.2)	9.0 (-0.3)	102.1 (76.1)	-5.6 (-4.5)

Due to the added noise, it is difficult to assess the true error in the recovered corrected signals. Therefore interpolated noise-free signals were simulated having correction factors calculated from various representative frequency errors. A DFT was performed on the corrected signals. The effects of the frequency errors on the harmonic amplitudes of the corrected signal are summarised in Table 2.

Table 2. Errors in harmonic amplitude in ppm of reading for various errors in frequency. For reasons of space only a representative set of harmonics results are shown.

Frequency error (ppm) \ Harmonic number	1	5	25	39	40
0	0.00	-0.02	-14.36	-88.60	-97.84
1	0.56	-2.77	-47.13	-158.4	-72.39
5	2.81	-14.10	-186.5	-457.9	8.23
10	5.58	-28.99	-379.1	-877.6	61.42
50	26.60	-177.7	-2662	-6060	-1415
100	49.92	-437.7	-7384	-17186	-8068

As can be seen from the tables, some of the cost functions can provide an accurate estimate of the deviation in the sampling rate from ideal and the signals can be corrected to sufficient accuracy under certain conditions. The performance is considerably worse under conditions of high noise. For example, a 50 ppm error in estimated frequency would result in an error of -6060 ppm for the 39th harmonic, as can be seen from Table 2. The frequency error of 67.3 ppm, which results when using cost function 3.2 for a noise level of 10 %, would therefore result in an error worse than -6060 ppm.

The accuracy is similar for other types of waveform,

although the cost functions that perform well here may not do so in other cases. For example, when using cost function 3.1 or 3.3, with the same settings used here, for an undistorted sine wave, the frequency error with a 10 % noise level is around 40 ppm regardless of whether interpolation is used or not. This leads to an error of around 20 ppm in the fundamental amplitude. The development of an appropriate cost function that is sufficiently robust to noise for a larger range of signals is ongoing.

4.2 Results with real signals

In order to assess the synchronisation methods under more realistic conditions two signals from two different voltage sources were used. The signals were sampled using a 24-bit ADC with a bandwidth of 60 kHz. For the synchronous case the sampling clock was set to 25 600 Hz, giving 512 samples per cycle for a 50 Hz waveform. For the asynchronous case the sampling rate was set to 25 817.9175 Hz, giving an apparent frequency of approximately 49.577972352 Hz. As above 20 cycles are used for the analysis.

The first signal was a nominally 50 Hz sine wave. This signal was first produced using a high quality source ("Source 1") that was phase-locked to the sampling clock of the measurement system. The signal is stable in amplitude, but the synchronisation is affected slightly by the frequency variation of the source due to imperfections in the phase-lock mechanism. This signal was also generated using the ARB ("Source 2") described below.

The second signal was a nominally Class A waveform as described in Section 4.1, again with a nominal frequency of 50 Hz. This signal was generated using Source 2, which had multiple channels. In this case the sampling clock for the ADC was supplied using a separate channel of Source 2. As such the sampling clock and the frequency of the generated waveforms were well synchronised. Source 2 is known to have relatively poor phase and amplitude stability and was chosen for this purpose.

The reliability of the correction technique and cost function is affected by the phase and amplitude stability of the signal sources. A Short Time Fourier Transform (STFT) was used to measure the phase variation with time of the fundamental component for both sources. An example of this variation for Source 2 is shown in Figure 2.

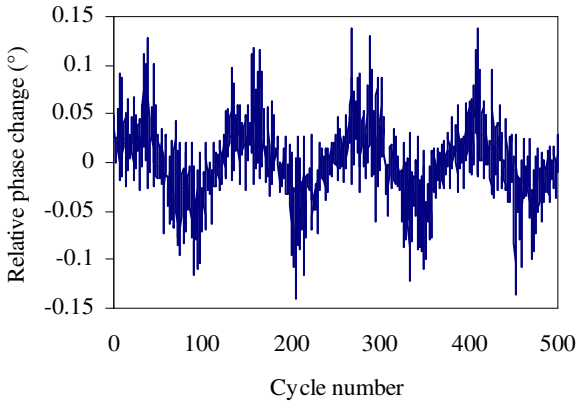

Fig. 2. Phase variation of fundamental for ARB

As can be seen in Figure 2, the phase of the waveform from Source 2 is subject to random variations and to slow variations that are probably mains beat. Source 1 is also subject to some random variations and mains beat, but this is approximately a factor of 100 smaller.

Five tests were performed using each of the cost functions defined in Section 3 for the two waveforms for the synchronous and asynchronous cases. 10 measurements were made and averaged to give the results for each case.

The differences in estimated frequency from the nominal assumed frequency, obtained with each of the cost functions, are given in Table 3 for the synchronous and asynchronous cases. The standard deviations from the 10 measurements are shown in brackets.

Table 3. Frequency errors in ppm for synchronous and asynchronous cases.

Signal type \ Cost function	3.1	3.2	3.3	3.4	3.5
Synchronous case					
Sine wave (Source 1)	-0.02 (0.17)	-0.03 (0.17)	-0.02 (0.17)	-0.03 (0.17)	-0.03 (0.17)
Sine wave (Source 2)	0.29 (0.99)	0.43 (0.64)	0.30 (0.97)	0.84 (1.52)	0.43 (0.64)
Class A (Source 2)	0.02 (0.10)	-1.31 (5.43)	0.03 (0.11)	-1.46 (6.49)	-0.05 (0.17)
Asynchronous case					
Sine wave (Source 1)	-0.02 (0.13)	-0.03 (0.13)	-0.02 (0.13)	-0.03 (0.13)	-0.03 (0.13)
Sine wave (Source 2)	-0.93 (1.55)	0.01 (1.13)	-0.92 (1.56)	0.01 (1.22)	0.01 (1.13)
Class A (Source 2)	0.01 (0.08)	-0.62 (3.75)	0.01 (0.08)	-3.06 (3.31)	-0.04 (0.26)

As can be seen from Table 3, the apparent quality of the frequency estimate is clearly affected by the input waveform. For the relatively stable undistorted sine wave generated with Source 1, the method gives fairly similar results with all five cost functions. There is some variation in frequency with time, which is probably largely due to the frequency variation in the source due to imperfect phase locks to the clock signal. Much of the standard deviation can most likely be attributed to this variation, as results with the five cost functions agree within 0.03 ppm for the majority of the 10 measurements.

For the noisier but well synchronised Class A waveform, the results have larger differences. The phase drift (3.2) and fundamental sidebands (3.4) cost functions are particularly adversely affected, also having a higher standard deviation than the other cost functions. This is to be expected given the phase and amplitude modulation of the waveform.

The lower errors and standard deviations of the Class A waveform results with cost functions 3.1 and 3.3 may indicate that they are more applicable to waveforms of this type, which have some degree of modulation. They are not so affected by phase variations as cost function 3.2 and are unlikely to be as adversely affected by amplitude variations as cost functions 3.4 and 3.5. Cost functions 3.1 and 3.3 are, however, more computationally intensive and perform

poorly under noisy conditions when the level of harmonic distortion is low. This can be seen in the results for the sine wave when generated with Source 2. All five cost functions give a similar performance with this waveform.

Also, the presence of interharmonics is not tested for here, but cost function 3.1 would be more likely to perform worse under those conditions.

As with the simulated results, a DFT was performed on the corrected waveform from the asynchronous measurements and on both the corrected and uncorrected waveforms from the synchronous measurements to determine the effect of frequency errors on the harmonics. For the sine wave generated with both sources, the corrected asynchronous measurements were in agreement with the synchronous measurements within the standard deviation (<10 ppm for Source 1 and around 200-300 ppm for Source 2). The results for the synchronous case for the Class A waveform are shown in Table 4. The results show the difference between the DFT of the uncorrected and corrected synchronised waveform.

Table 4. Differences in harmonic amplitude in ppm of reading. For reasons of space only a representative set of harmonics results are shown.

Harmonic number / Cost function	1	5	25	39	40
Synchronous case					
3.1	0.1	0.1	1.8	2.5	-2.4
3.2	-4.5	-3.2	-72.8	-96.5	69.7
3.3	0.1	0.1	2.0	2.8	-2.6
3.4	-5.5	-9.5	-147.1	-220.8	123.3
3.5	0.0	0.2	3.1	4.6	-3.5

In the synchronous case the differences refer to the same waveform and are therefore not affected by the standard deviation of the measurements, only the frequency estimate and correction technique. The frequency errors for cost functions 3.2 and 3.4 can be seen to have a significant effect, which is comparable to the typical simulated errors in Table 2. For the asynchronous case all the corrected results agree with the synchronous results within the standard deviation (around 400-500 ppm for the fundamental). This could lead one to believe that the cost functions and correction technique are good enough for the signals presented. However, though of poor quality from a laboratory metrology point of view, this signal is still relatively benign compared to those arising on the electricity supply network and the observed differences in frequency estimates could have greater implications for different waveforms.

6. CONCLUSIONS

The described algorithm works well for measurements in controlled conditions where noise levels are low and the waveforms are stable and stationary. The performance of the algorithm under various conditions is determined by the choice of cost function to assess the degree of synchronisation. The cost functions used in the analysis presented in this paper work well for certain signals, but are not ideal under noisy conditions or where the signals are subject to large amplitude and phase variations. Further work is required to find a cost function appropriate for power quality measurements that copes under these more demanding conditions.

ACKNOWLEDGMENTS

This work was supported within the UK DIUS National Measurement System Policy Unit's Program for Electrical Metrology and partially funded by European Community's Seventh Framework Programme, ERA-NET Plus, under Grant Agreement No. 217257.

REFERENCES

[1] *Electromagnetic Compatibility (EMC) – Testing and measurement techniques – Part 4-30: Power Quality Measurement Methods*, *IEC 61000–4–30*, Published by The International Electrotechnical Commission, 2003.

[2] Jing Wu and Wei Zhao, "New Precise Measurement Method of Power Harmonics Based on FFT", *Proc. International Symp. Intel. Sig. Proc. and Comm. Sys.*, pp. 365-368, Dec. 2005.

[3] Fusheng Zhang, Zhongxing Geng and Wei Yuan, "The Algorithm of Interpolating Windowed FFT for Harmonic Analysis of Electric Power System", *IEEE Trans. Power Del.*, vol.16, nº. 2, pp. 160-164, Apr. 2001.

[4] D. J. Nyarko and K. A. Stromsmoe, "A Modified DFT for Improved Accuracy in Harmonic Measurements of Periodic Waveforms", *Canadian Conference on Electrical and Computer Engineering*, vol. 2, pp. 708-711, 1996.

[5] LiMin Zhu, Han Ding and Xiang Yang Zhu, "Extraction of Periodic Signal Without External Reference by Time-Domain Average Scanning", *IEEE Trans. Ind. Electron.*, vol. 55, No. 2, pp. 918-927, Feb. 2008.

[6] W. G. K. Ihlenfeld, "Simple Algorithm for Sampling Synchronization of ADCs", *CPEM 2008 Conference Digest*, pp. 676-677, Broomfield, Colorado, June 2008.

[7] M. F. da Silva, P. M. Ramos, A. C. Serra, "Simulation and Experimental Results of Multiharmonic Least-Squares Fitting Algorithms Applied to Periodic Signals", *Measurement*, vol. 35, No. 2, pp. 131-137, Mar. 2004.

[8] M. F. da Silva, P. M. Ramos, A. C. Serra, "A New Four Parameter Sine Fitting Technique", *IEEE Trans. Instrum. Meas.*, vol. 55, No. 2, pp. 646-651, Apl. 2006.

[9] W. H. Press, S. A. Teukolsky, W. T. Vetterling and B. P. Flannery, *Numerical Recipes in C: The Art of Scientific Computing*, Cambridge University Press, Cambridge, 1992.

[10] R. G. Baraniuk, P. Flandrin, A. J. E. M. Janssen, and O. Michel, "Measuring time-frequency information content using the Rényi entropies", *IEEE Trans. on Info. Theory*, vol. 47, no. 4, pp. 1391–1409, May 2001.

[11] National Physical Laboratory, "NPL Power Quality Waveform Library", [Online], accessed 27 May 2009, http://resource.npl.co.uk/waveform/datafiles/harmonics_service_class_a.xml.

[12] *Electromagnetic Compatibility (EMC) – Part 3-2: Limits – Limits for Harmonic Current Emissions (Equipment Input Current ≤ 16 A per Phase), IEC 61000–3–2*, Published by The International Electrotechnical Commission, 2005.